

On the Reactions of Ca_n^+ , Sr_n^+ , and Ba_n^+ with Water and Alcohols

Victor A. Mikhailov, Glen Akibo-Betts, and Anthony J. Stace*

The School of Chemistry, Physics, and Environmental Sciences, The University of Sussex, Falmer, Brighton, BN1 9QJ, U.K.

Received: May 1, 2002

The reactions of metal cluster ions, M_n^+ , with water and alcohols, where M^+ is calcium ($n = 1-7$), strontium ($n = 1-6$), or barium ($n = 1-4$), have been studied using a pulsed arc cluster ion source (PACIS) in association with a Finnigan ion trap. The dominant reaction products with water are found to have the general formula $\text{M}_n^+(\text{OH})_{2n-1}$, which can be attributed to M^+OH in association with $(n-1)$ neutral $\text{M}(\text{OH})_2$ species. Other products present in the trap include $\text{M}_n^+\text{O}_p(\text{OH})_q$ cluster ions covering a range of values for n , p , and q . A few $\text{M}_n^+(\text{OH})_{2n-1}$ and $\text{M}_n^+\text{O}_p(\text{OH})_m$ ions respond to collisional activation, but the majority of complexes are found to be reluctant to fragmentation. The reactions of individual $\text{M}_n^+(\text{OH})_{2n-1}$ complexes have been studied in the presence of methanol, ethanol, and 1-propanol, and the results have been interpreted in terms of the sequential exchange of hydroxyl groups for MeO, EtO, and PrO, respectively. A general formula for these reactions is proposed to be $\text{M}_n^+(\text{OH})_{2n-1} + m(\text{ROH}) \rightarrow \text{M}_n^+(\text{OH})_{2n-m-1}(\text{RO})_m + m(\text{H}_2\text{O})$, where ROH is the alcohol, the final products being $\text{M}_n^+(\text{MeO})_{2n-1}$, $\text{M}_n^+(\text{EtO})_{2n-1}$, and $\text{M}_n^+(\text{PrO})_{2n-1}$. Supporting calculations suggest possible candidate structures for two of the $\text{M}_n^+(\text{OH})_{2n-1}$ ions; however, neither provides an obvious route to the complete exchange of OH for OR.

I. Introduction

Reactions between metal cluster ions and large numbers of solvent molecules ($\text{M}_n^+ - n\text{L}$ reactions) are of particular interest because the presence of molecules coordinated to an underlying metal cluster should reflect the chemical and geometrical properties of M_n^+ . It has been known for some time that polynuclear ionic metal species exist in solution;¹ therefore, studies of their chemistry should provide valuable information that may reflect the transition from gas-phase to condensed-phase reactivity. Although numerous studies have been undertaken of gas-phase reactions of monatomic metal ions with solvent molecules, other than studies of coordination, equivalent experiments on the chemistry of metal cluster ions with more than one solvent molecule are scarce.

Comparisons of the gas-phase chemistry exhibited by alkaline earth metal atoms are worthy of consideration because these metals, excepting beryllium, are known to react extensively with water and alcohols in the bulk liquid phase. In addition, monatomic ions of the metals have been found to react with clusters of water and methanol in molecular beam experiments.²⁻⁶ The reactions of monatomic ions of magnesium,^{2,4} calcium,^{3,5} and strontium⁶ with water have all been observed to follow a similar pathway:



for $4 < n < 16$ for $\text{M} = \text{Mg}$ and Ca and $n > 5$ for $\text{M} = \text{Sr}$. Supporting ab initio calculations^{4,5,7} have shown that the switch in reaction product from $\text{M}^+(\text{H}_2\text{O})_n$ to $\text{M}^+\text{OH}(\text{H}_2\text{O})_{n-1}$ at $n = 5$ occurs because polarization of the hydroxide ion gives M^+OH a higher hydration energy than M^+ .

Lu and Yang⁸ have studied the reactions of alkaline earth metal ions with methanol and have also observed hydrogen

elimination. For Mg^+ , it led to a switch from $\text{Mg}^+(\text{MeOH})_n$ to $\text{Mg}^+\text{MeO}(\text{MeOH})_{n-1}$ for $4 < n < 16$, which is very similar to that observed for water. In the reactions of Ca^+ , Sr^+ , and Ba^+ with methanol, the association product $\text{M}^+\text{CH}_3\text{OH}$ was found together with M^+OCH_3 and M^+OH . Ab initio calculations on $\text{Mg}^+(\text{MeOH})_n$ and $\text{Mg}^+\text{MeO}(\text{MeOH})_{n-1}$ demonstrated that, similar to Mg^+OH , the switch between product ions is driven by a higher degree of polarization in Mg^+OCH_3 and a corresponding increase in solvation energy. However, no satisfactory explanation could be given for similar product ion switches seen for Ca^+ , Sr^+ , and Ba^+ .

In extending these observations to the reactivity of metallic clusters, it is not obvious that their behavior can be deduced simply from the behavior of atomic ions. Transitions of structural and electronic properties are to be expected as clusters increase in size. Lu and Yang have reported limited results on the reactivity of Mg_2^+ in that they observed $\text{Mg}_2^+(\text{MeO})_2(\text{MeOH})_{n-2}$ and $\text{Mg}_2^+(\text{MeO})_3(\text{MeOH})_{n-3}$ as fragments in their experiments.⁸ Earlier we reported on a study of the reactions of barium clusters ions, Ba_n^+ , with water.⁹ These reactions could not always be equated with the formal oxidation number of the barium atom, and it was observed that the number of hydrogen atoms eliminated from water varied from $2n - 1$ for $n < 4$ to $2n + 1$ for $n = 4$ and $2n + 2$ for $n = 5$, leading to the formation of $\text{Ba}_4^+\text{O}_4\text{OH}(\text{H}_2\text{O})_{m+1}$ and $\text{Ba}_5^+\text{O}_6(\text{H}_2\text{O})_{m+2}$, respectively. Because barium clusters readily form oxides and hydroxides in reactions with water, clusters of the form Ba_nO_m can be expected to constitute the core of many of the reaction products involving oxygen-containing molecules. Chevaleyre and co-workers¹⁰ undertook an extensive study of the ionization energies of Ba_nO_m ($1 < n < 14$, $m \leq n$) and found a rapid transition to the bulk ionic structure for stoichiometric $(\text{BaO})_n$ clusters. However, no data on Ba_nO_m clusters with $m > n$ have been reported in the literature.

In this paper, we present results from a study of the reactions of small ionic clusters of the metals Ca, Sr, and Ba with water

* Corresponding author. E-mail: A.J.Stace@sussex.ac.uk. Tel: 44-1273 606 755. Fax: 44-1273 677 196.

in a pulsed arc cluster ion source (PACIS) and subsequent reactions of the ionic metal hydroxide clusters with the alcohols CH_3OH , $\text{C}_2\text{H}_5\text{OH}$, and $\text{C}_3\text{H}_7\text{OH}$. The latter experiments were performed on metal hydroxide clusters held in an ion trap (Paul or ICR), which provides a convenient means of storing ions for time periods ranging from a few milliseconds to minutes. During that time, cluster ions produced in a PACIS can undergo structural rearrangement and cooling (either collisional or radiative) prior to undergoing further chemical processes. Additional advantages of ion trapping are the capability for multistep (MS)^{*m*} ion selection and the ability to promote collision-induced dissociation (CID) and photofragmentation of ion complexes.^{11–16}

II. Experimental Section

The apparatus combines a pulsed arc cluster ion source (PACIS), a quadrupole ion trap (Finnigan, ITMS), and an electrostatic ion guide designed for delivering ions from the PACIS to the trap. Detailed descriptions of the PACIS and Finnigan ion trap have been given elsewhere,^{9,15,16} and just a brief description is provided here. Samples of calcium, strontium, and barium (lumps, Sigma-Aldrich, 99% purity) used in the PACIS were held in a stainless steel cup and taken as the negative electrode. The positive electrode consisted of a short rod of oxygen-free copper. Two techniques were tested for promoting association reactions between monatomic or cluster metal ions and solvent molecules. In the first method, helium (BOC Gases, Research Grade) was passed through an in-line reservoir containing water prior to entering a fuel injector that provided gas/vapor pulses of approximately 1-ms duration. This composite carrier gas was then entrained with metal vaporized by a pulsed arc, and the resultant mixture then underwent adiabatic expansion into a vacuum. In a second approach, which gave more reliable signals, a few drops of water were frozen to the surface of the exit to a liquid nitrogen-cooled extender, which acted as part of the collimation arrangement for the PACIS. As the helium/metal vapor passed over the ice, a small amount of water was liberated from the surface to become associated with the metal complexes. Ion transmission between the PACIS and the ion trap was facilitated using an ion guide, which was designed according to details outlined in ref 17 and has a total length, including entrance and exit lenses, of approximately 50 cm. The design of the guide was optimized by simulating ion trajectories using the SIMION 6.00 package. To facilitate the passage of ions from the guide into the trap, it was necessary to apply a small negative DC voltage to the end electrodes of the trap.

To study the chemistry of particular ion/solvent combinations, ions of a particular mass were isolated within the trap and subjected to collisional excitation. Effective operation of the trap requires the presence of a background gas pressure, which is normally helium held at a pressure in the range 10^{-5} – 10^{-4} Torr. Therefore, collisional excitation of trap ions could be achieved by influencing their motion through the application of an AC voltage to the end electrodes. As the kinetic energy of the ions increases, they gain internal excitation through collisions with the helium buffer gas. Use of the latter in the trap proved particularly convenient because helium was also used in the PACIS; therefore, there was no need for extensive differential pumping in the expansion process. The final detection of ions was accomplished by their ejection from the trap through one of the end caps in the direction of a conversion dynode and electron multiplier. The upper mass range of the trap was 650 amu, and under most operating conditions, unit mass resolution could be achieved.

In routine operation, the ion trap is normally heated to a temperature of 100 °C to help eliminate any background water vapor. However, even with heating and the use of a liquid nitrogen trap on the helium inlet, there was often sufficient residual water to promote reactions with alkaline earth metal ions, particularly if the latter are held in the trap for longer than 10 ms.

III. Computational Details

To provide insight into the structure and stability of some of the complexes studied in the experiment, the $[\text{Ca}_n(\text{OH})_m]^+$ system was investigated by DFT methods. This particular example was chosen to minimize computational effort because calculations on complexes containing Sr and Ba would be more likely to require extensive relativistic corrections. Complexes of the general form $\text{Ca}^+\cdot\text{X}_m$ have been studied before at the DFT level of theory, and the results have been shown to be in reasonable agreement with high-level ab initio theory. DFT studies of Ca_n clusters¹⁸ found that for the calcium dimer the exchange functional in the generalized gradient approximation (GGA) scheme overestimates the binding energy. This tendency has been reported for other systems including neutral, monocationic, and dicationic complexes;¹⁹ however, this bias has not been shown to lead to deviations from minimum-energy geometries. Results also give accurate representations of the bonding interactions in the species studied, and in the aforementioned investigations, the $\text{Ca}^+\cdot\text{X}_m$ interactions are reported as being primarily of an electrostatic nature. Our aim was to calculate the most stable structures of the complexes concerned and to ascertain their binding energy with respect to the species we consider to be component building blocks of the complex series, namely, $[\text{CaOH}]^+$ and $[\text{Ca}(\text{OH})_2]$.

Calculations were performed using a density functional theory (DFT) program implemented in the Amsterdam density functional (ADF2000.01) package initially developed by Baerends et al.²⁰ The calculations employed Slater-type orbitals as basis sets, and the electron spins of the systems were kept restricted. Geometry optimizations used the local density functional formulas given by Vosko, Wilk, and Nusair (VWN),²¹ and GGA were applied after the calculation of SCF wave functions. The ADF program suite utilizes the exchange gradient correction of Becke²² (88), and the correlation gradient corrections as given by Perdew²³ (86), also known as BP86, were implemented throughout the calculations. For the $[\text{Ca}_n(\text{OH})_{2n-1}]^+$ systems, the atomic orbitals on Ca were described by a triple- ζ Slater function basis set, whereas a double- ζ Slater function basis set with polarization was used for oxygen and hydrogen. The $1s^2$ configuration on O was treated as the core and represented by the frozen core approximation, as was the $2p^6$ configuration on Ca.

To avoid finding saddle points rather than true minima, symmetry constraints were neglected for all starting points of the geometry optimization calculations. Once suitable structures had been identified, symmetry constraints were imposed to further optimize structures and obtain true minima. Minimum-energy structures were confirmed by calculating harmonic frequencies from force constants in ADF by numerical differentiation of energy gradients in slightly displaced geometries.²⁴

IV. Results and Discussion

A. M_n^+ and Water Reactions. The first objective was to determine which types of complexes between alkaline earth metal ions and water could be formed and trapped using the

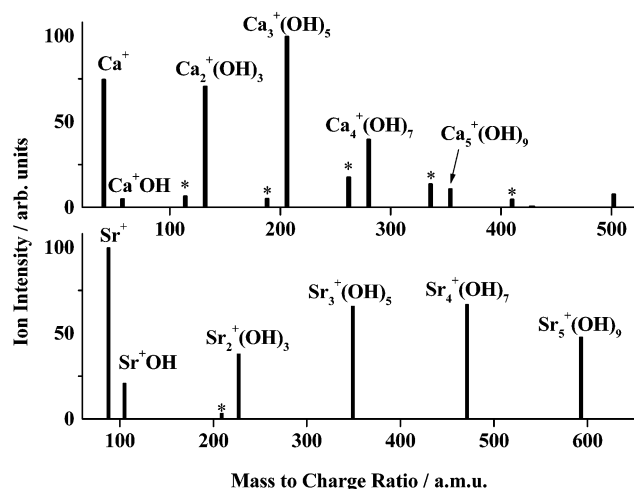


Figure 1. Products from the reactions of Ca_n^+ and Sr_n^+ with water vapor, seeded in the carrier gas. Asterisk (*) labels denote $\text{M}_n^+\text{O}(\text{OH})_{2n-3}$. The peak at 501 amu is probably related to $\text{Ca}_7^+(\text{OH})_{13}$.

PACIS. Injecting helium saturated with water vapor at room temperature into the PACIS failed to produce any form of complex; however, by gradually reducing the water content of the rare gas flow, the results shown in Figure 1 for calcium and strontium were obtained. For an easier perception of acquired mass spectra, only the ion peaks of major isotopes for every n are plotted in all subsequent figures. Once optimum conditions were achieved, the resultant spectra proved to be very persistent and highly reproducible. The most striking feature of the mass spectra is their periodicity, which can be related to the sequential addition of neutral hydroxide $\text{M}(\text{OH})_2$ molecules. For strontium, the mass spectrum is dominated completely by what should be considered to be $\text{Sr}_n^+(\text{OH})_{2n-1}$ complexes. For calcium, the dominant ions present in the mass spectra can be attributed to the combinations of $\text{Ca}_n^+(\text{OH})_{2n-1}$ and $\text{Ca}_n^+\text{O}(\text{OH})_{2n-3}$. For barium, a similar enhancement of $\text{Ba}_n^+(\text{OH})_{2n-1}$ ions for $n = 2$ and 3 could be found; however, there were also other ions present that reflected alternative reaction pathways with water (see below). The validity of assigned ion compositions will be discussed later; however, it should be noted that the structure of $\text{M}_n^+(\text{OH})_{2n-1}$ complexes is stoichiometric for Group 2A elements, and as a first approximation, they could be considered to be composed of one M^+OH ion and a few $\text{M}(\text{OH})_2$ molecules. It is presumed that ionic hydroxides are formed by pulsed arc evaporation and ionization of the bulk hydroxides, which are formed on the surface of the electrodes by the reaction between water vapor in the helium flow and the bulk metal.

In contrast to the approach used to generate the ions seen in Figure 1, Figure 2 shows mass spectra recorded from ions produced when vaporized strontium or barium reacts with water that has been frozen in the extender. It can be seen that, although stoichiometric hydroxide cluster ions $\text{M}_n^+(\text{OH})_{2n-1}$ are among the observed reaction products in Figure 2, the whole spectrum is far more complicated. The complete range of observed strontium-containing complexes is given in Table 1, and we shall discuss these first before returning to an analysis of the data on Ca_n^+ and Ba_n^+ complexes.

The variety of species observed in Figure 2a and listed in Table 1 could be formed either from the fragmentation of larger oxide or hydroxide complexes ablated directly from the electrode surface in PACIS or by the reactions of Sr_n^+ with increasing numbers of water molecules. In support of the latter route to hydroxide cluster formation, it is found that when Sr_2^+ was

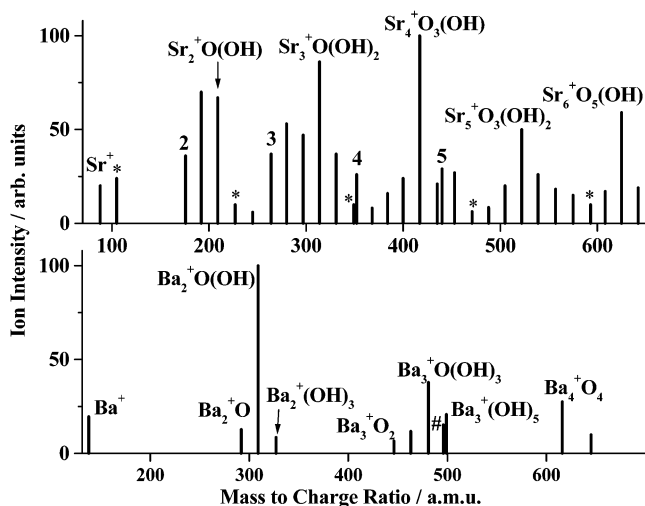


Figure 2. Products from the reactions of Sr_n^+ and Ba_n^+ with water molecules picked up in the extender. Asterisk (*) labels denote $\text{Sr}_n^+(\text{OH})_{2n-1}$ ions, and $n = 2-5$ identifies bare Sr_n^+ clusters. Hash (#) labels denote the $\text{Ba}_3^+\text{O}_4(\text{H}_2\text{O})$ complex.

TABLE 1: Products from Sr_n^+ Reaction with Water

Sr_2^+	Sr_3	Sr_4^+	Sr_5^+	Sr_6^+O_5
Sr_2^+O	Sr_3^+O	Sr_4^+O	Sr_5^+O_3	$\text{Sr}_6^+\text{O}_5\text{OH}$
$\text{Sr}_2^+\text{O}(\text{OH})$	$\text{Sr}_3^+\text{O}(\text{OH})$	Sr_4^+O_2	$\text{Sr}_5^+\text{O}_3\text{OH}$	
$\text{Sr}_2^+(\text{OH})_3$	$\text{Sr}_3^+\text{O}(\text{OH})_2$	Sr_4^+O_3	$\text{Sr}_5^+\text{O}_3(\text{OH})_2$	
$\text{Sr}_2^+(\text{OH})_3\text{H}_2\text{O}$	$\text{Sr}_3^+\text{O}(\text{OH})_3$	$\text{Sr}_4^+\text{O}_3\text{OH}$	$\text{Sr}_5^+\text{O}_3(\text{OH})_3$	
	$\text{Sr}_3^+(\text{OH})_5$	$\text{Sr}_4^+\text{O}_2(\text{OH})_3$	$\text{Sr}_5^+\text{O}_2(\text{OH})_5$	
		$\text{Sr}_4^+\text{O}(\text{OH})_5$	$\text{Sr}_5^+\text{O}(\text{OH})_7$	
		$\text{Sr}_4^+(\text{OH})_7$	$\text{Sr}_5^+(\text{OH})_9$	

isolated in the trap and allowed to react with residual water vapor, limited reactivity was observed, leading to Sr_2^+O and $\text{Sr}_2^+\text{O}(\text{OH})$ after 5-ms of trapping time (Figure 3a). When the trapping time was increased to 105 ms, the overall abundance of the reaction products increased, and in addition to the two reaction products given above, a new ion, $\text{Sr}_2^+(\text{OH})_3$, appears in the mass spectrum (Figure 3b). However, given the persistence of the pattern in Figure 1, we would propose that some of the clusters observed in Figure 2 have been formed via the fragmentation of large hydroxide complexes that have evaporated from the bulk metal surface.

To help establish the structures of the complexes with Sr_n^+ , an attempt was made to promote reactivity via collisional activation. The only hydroxide complex found to respond to collisions was $\text{Sr}_2^+(\text{OH})_3$, which produced $\text{Sr}_2^+\text{O}(\text{OH})$ as a fragment. However, even that step was observed only through the use of a collision partner (neon) heavier than helium as the trap background gas. $\text{Sr}_2^+\text{O}(\text{OH})$ was subsequently found to fragment to Sr^+OH . All other complexes were reluctant to fragment even in the presence of neon.

Several of the complexes identified in Figure 2 would appear to owe their appearance to the fact that reactivity has taken place in the presence of restricted numbers of water molecules. In assigning compositions to the ions in Figures 1 and 2, chemical formulas have been chosen that contain no adducted water molecules. This assumption is supported by the reluctance of complexes to fragment under collisional activation. In the case of both calcium and strontium, the dissociation energy of M^+OH is much higher than that of $\text{M}^+\text{H}_2\text{O}$.^{25,26} The Sr^+OH bond energy is 4.67 eV (450 kJ/mol), whereas the Sr^+OH_2 bond energy is just 104 kJ/mol. A similar difference in binding energies should be expected for cluster ions of the Group 2A metals. If, for example, strontium-containing ions were of the

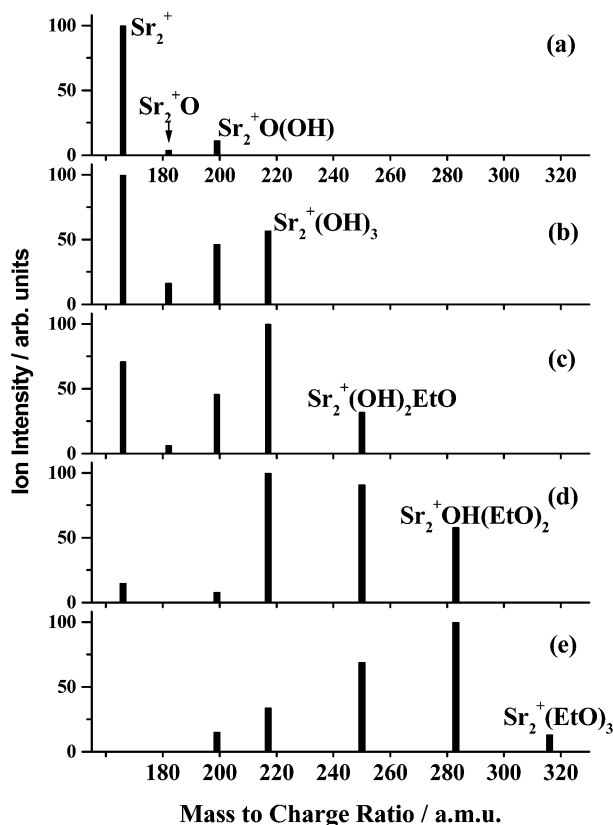


Figure 3. Evolution of ion populations in the trap: (a) isolation of Sr_2^+ , trapping time 5 ms; (b) trapping time 105 ms; (c), (d), and (e) introduction of d_5 -EtOD via a Jordan nozzle into the trap containing Sr_2^+ , reaction time 105 ms. The concentration of d_5 -EtOD increases from (c) to (e).

form $\text{Sr}_4^+\text{O}_3\text{OH}(\text{H}_2\text{O})_2$ rather than $\text{Sr}_4^+\text{O}(\text{OH})_5$, then collisions would be expected to remove one or both of the water molecules.

A difference in composition is clearly observed between Sr_n^+ complexes with even values of n (2 and 4) and those with odd values (3 and 5). When n is even, an increase in the number of water molecules available for reaction leads to a series that follows a progression starting from $\text{Sr}_n^+\text{O}_{n-1}$, passing through $\text{Sr}_n^+\text{O}_{n-1}\text{OH}$, and eventually resulting in the formation of $\text{Sr}_n^+(\text{OH})_{2n-1}$. Although it falls outside of the mass range, it is assumed that a similar sequence exists for $n = 6$ because Sr_6^+O_5 and $\text{Sr}_6^+\text{O}_5\text{OH}$ are observed. When n has odd values, the sequence of the products is quite different. Oxides are formed up to $\text{Sr}_n^+\text{O}_{n-2}$, and then further reactivity with water follows a sequence through $\text{Sr}_n^+\text{O}_{n-2}(\text{OH})_m$ ($m = 1-3$) complexes, eventually stopping once $\text{Sr}_n^+(\text{OH})_{2n-1}$ ions are formed. The series from $\text{Sr}_n^+\text{O}_{n-1}\text{OH}$ to $\text{Sr}_n^+(\text{OH})_{2n-1}$ in the case of even-sized Sr_n^+ and from $\text{Sr}_n^+\text{O}_{n-2}(\text{OH})_3$ to $\text{Sr}_n^+(\text{OH})_{2n-1}$ in the case of odd-sized clusters can be related to the stoichiometric composition of strontium oxides and hydroxides.

The case for calcium seems somewhat different from that of strontium. Both $\text{Ca}_n^+(\text{OH})_{2n-1}$ and $\text{Ca}_n^+\text{O}(\text{OH})_{2n-3}$ ($n < 7$) are present in the mass spectra in Figure 1, and the relative abundance of the latter increases with n . The precise identities of complexes that have masses > 430 amu are unclear. When the trapping time is increased up to 200 ms, which corresponds to a longer period of reaction with residual water vapor in the trap, the intensities of $\text{Ca}_n^+(\text{OH})_{2n}$ ions increase with respect to those with the composition $\text{Ca}_n^+\text{O}(\text{OH})_{2n-3}$ ($n < 6$). It proved impossible to obtain Ca_n^+ complexes containing less oxygen than the combinations seen in Figure 1. Even after long periods

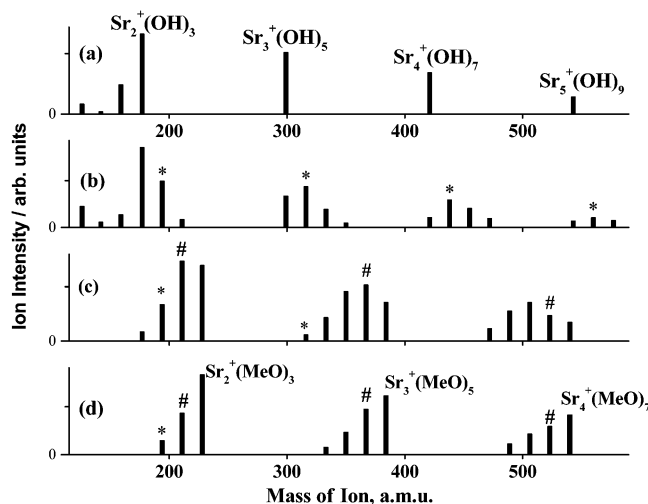


Figure 4. Evolution of ion populations in the trap: (a) initial populations of the hydroxide clusters; (b), (c), and (d) introduction of d_3 -MeOD into the trap via a Jordan nozzle, reaction time 105 ms. The concentration of d_3 -MeOD increases from (b) to (d). Asterisk (*) labels denote $\text{Sr}_n^+(\text{OH})_{2n-2}\text{MeO}$ clusters, and hash (#) labels denote $\text{Sr}_n^+\text{OH}(\text{MeO})_{2n-2}$.

of arcing with pure, dry helium, the distribution remained constant. We believe the samples of calcium to contain significant amounts of $\text{Ca}(\text{OH})_2$ prior to their use in the experiment.

Following collisional activation, $\text{Ca}_n^+(\text{OH})_{2n-1}$ ions were found to fragment only to $\text{Ca}_n^+\text{O}(\text{OH})_{2n-3}$. In turn, $\text{Ca}_n^+\text{O}(\text{OH})_{2n-3}$ ions were reluctant to fragment further. The CID data imply that $\text{Ca}_n^+(\text{OH})_{2n-1}$ clusters may easily adopt an alternative composition, such as $\text{Ca}_n^+\text{O}(\text{OH})_{2n-3}\text{H}_2\text{O}$, that can readily lose a water molecule. The trap mass spectra suggest that water loss is quite facile in the calcium-containing complexes and increases in probability as a function of n , at least for $n < 7$. However, reactions of calcium complexes with deuterated alcohols support the proposed formula $\text{Ca}_n^+(\text{OH})_{2n-1}$ rather than the alternative $\text{Ca}_n^+\text{O}(\text{OH})_{2n-3}\text{H}_2\text{O}$ formula (see below).

Within the mass range accessible in the trap (0–650 amu), the products from Ba_n^+ /water reactions were found to be very similar to those observed in an earlier TOF/PACIS study of this system.⁹ The only exceptions were $\text{Ba}^+(\text{H}_2\text{O})_n$, Ba_2^+OH , and $\text{Ba}_2^+\text{O}(\text{H}_2\text{O})_n$, which had low intensities in the TOF mass spectra and were completely absent in the ion trap mass spectra. When water is deliberately omitted from the PACIS, ion peaks that could be related to $\text{Ba}_3^+\text{O}_4^+$ and $\text{Ba}_3^+\text{O}_4^+(\text{H}_2\text{O})$ are observed in the ITMS spectra. $\text{Ba}_2^+\text{O}(\text{OH})$ also appears in the spectra under these conditions, but $\text{Ba}_2^+(\text{OH})_3$ and $\text{Ba}_3^+(\text{OH})_5$ are not formed. For $n = 4$, the ions Ba_4^+O_4 and $\text{Ba}_4^+\text{O}_4(\text{H}_2\text{O})$ are observed, which is consistent with our earlier TOF measurements⁹ where $\text{Ba}_4^+\text{O}_4(\text{H}_2\text{O})_2$, $\text{Ba}_4^+\text{O}_4\text{OH}(\text{H}_2\text{O})_2$, and $\text{Ba}_4^+\text{O}_4(\text{H}_2\text{O})_m$ were also found.

A particular feature of the barium cluster–water results is that the numbers of oxygen atoms and hydroxide groups present in the products are larger than those that are appropriate for stoichiometric barium oxide and hydroxide clusters. One explanation for this behavior could be the tendency of barium to form the peroxide BaO_2 , which has a very high thermal stability and does not react with water.²⁷ Our observation of the formation of Ba_4^+O_4 in reactions of Ba_4^+ with water is consistent with the data of Chevaleyre and co-workers,¹⁰ who found $(\text{BaO})_4^+$ to be the dominant product following photodissociative ionization of a variety of barium oxide clusters. The latter fact is related to the particular stability of the neutral

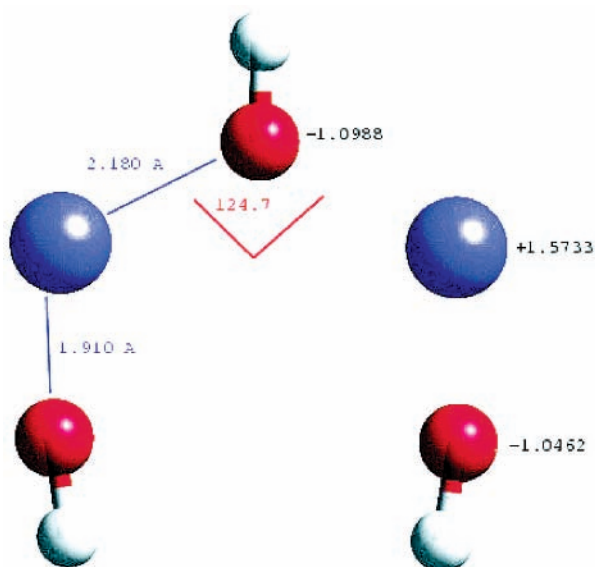


Figure 5. Structure calculated for $\text{Ca}_2^+(\text{OH})_3$ using the method outlined in the text.

$(\text{BaO})_4$ cluster, whose structure corresponds to a highly symmetric cubic structure.

All of the complexes shown in Figure 2b were resistant to fragmentation following collisional activation. As in the case of strontium, this result suggests that there are no adducted water molecules in the clusters. Some ions could have formulas that are different from those given in our earlier TOF study of this system⁹ (e.g., instead of $\text{Ba}_3^+\text{O}_2\text{OH}(\text{H}_2\text{O})_2$, we now believe a more realistic formula to be $\text{Ba}_3^+(\text{OH})_5$). These new assignments have been chosen in response to our current observations on stability and on the participation of strontium and barium hydroxides in the structures of the complexes. Although these alternatives will remain arbitrary until a complete study on the structure of these clusters is done, it is generally known that, excepting beryllium, alkaline earth metals and their oxides strongly favor the formation of hydroxides in reactions with water.²⁸ Reluctance of the hydroxide clusters to fragment at CID can be taken as indicative of very strong intermolecular forces being responsible for their presence. Further evidence in support of $\text{M}_n^+(\text{OH})_{2n-1}$ structures comes from their reactions with alcohol molecules.

The results highlight the existence of stable $\text{M}_n^+(\text{OH})_{2n-1}$ structures for which one possible interpretation suggests the presence of a $[\text{M}(\text{OH})]^+$ core. Felmy et al.²⁹ have discussed a similar ion core in structures calculated at the DFT level, and their accompanying experimental data were also interpreted in terms of the $[\text{Ca}(\text{OH})]^+$ ion playing a role in solution-phase chemistry. To better understand the experimental data presented above, structures have been calculated for the first two members of the $[\text{Ca}_n(\text{OH})_{2n-1}]^+$ series, namely, $[\text{Ca}_2(\text{OH})_3]^+$ and $[\text{Ca}_3(\text{OH})_5]^+$. The results are shown in Figures 5 and 6, where the optimized geometries, bond lengths, and bond angles are shown together with a Mulliken charge population analysis of each atom, which is given in brackets. Parts a and b of Figure 6 show different orientations of the same $[\text{Ca}_3(\text{OH})_5]^+$ structure. In isolation, the $[\text{Ca}(\text{OH})]^+$ unit is calculated to have a bond length of 1.852 Å. The trend in stabilization energy is $[\text{Ca}(\text{OH})]^+ < [\text{Ca}_2(\text{OH})_3]^+ < [\text{Ca}_3(\text{OH})_5]^+$ (i.e., one of increasing stability as the units increase in size). Unfortunately, it was not possible to perform calculations on systems where $n = 4$.

Analysis of the charge populations of each complex (numbers in parentheses) would suggest that the structures are very ionic,

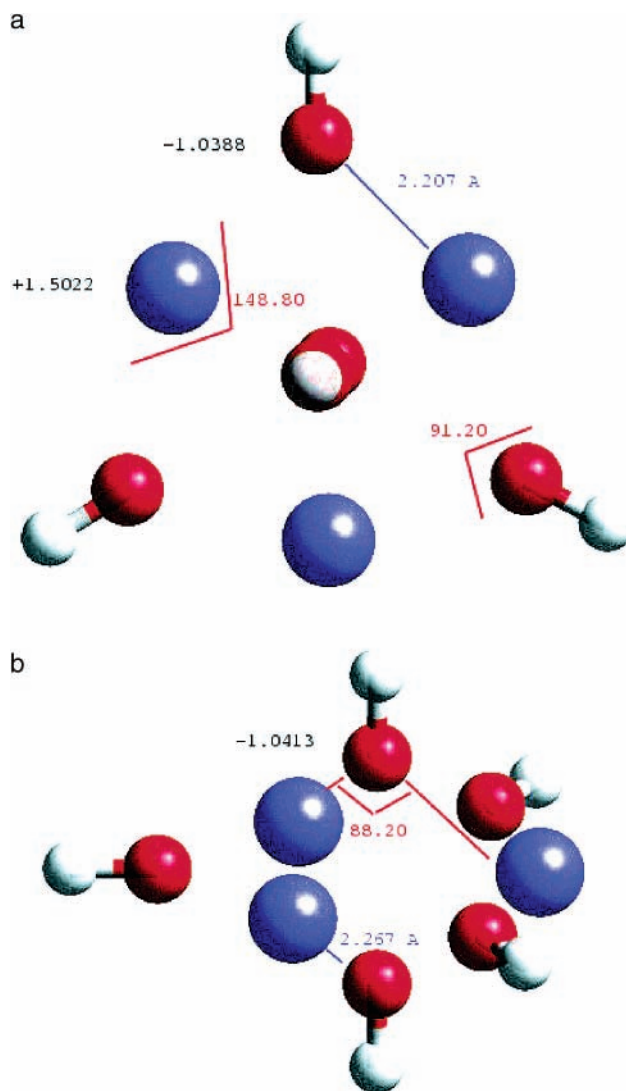


Figure 6. Two views of the structure calculated for $\text{Ca}_3^+(\text{OH})_5$ using the method outlined in the text.

with each Ca atom striving to achieve a charge of +2 and each O atom succeeding in acquiring a charge of -1. The structure calculated for $[\text{Ca}_2(\text{OH})_3]^+$ is comparatively open; in contrast, the $[\text{Ca}_3(\text{OH})_5]^+$ structure is a compact, almost cyclic unit similar to those seen for polynuclear cations in the bulk.³⁰ Likewise, the ability of OH^- to form a bridge between metal cations is very similar to behavior seen in the bulk.¹ These similarities between the calculated gas-phase structures and patterns of behaviour seen in hydrolyzed alkaline earth metals in the bulk would suggest that the structures shown in Figures 5 and 6 are reasonably realistic.

B. Reactions with Alcohols. A direct reaction between Group 2A metals and alcohols is possible but requires a catalyst. For example, magnesium alkoxides are readily formed in the presence of iodine:³¹



Ionic metal alkoxides, M^+OR , can be formed in gas-phase reactions of monatomic Group 2A metal ions with alcohols.⁸ In the trap, we have observed the formation of M^+OR and $\text{M}^+\text{-OR}(\text{ROH})_m$ complexes in reactions of Ca^+ , Sr^+ , and Ba^+ with alcohols, and for strontium, Sr^+ROH complexes were also formed. The abundance of Sr^+MeOH ions was lower than that of Sr^+MeO , Sr^+EtOH , and Sr^+EtO ions, all of which had almost

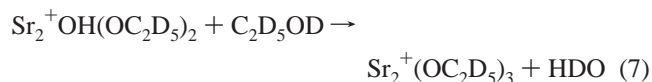
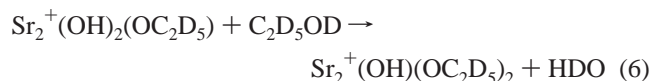
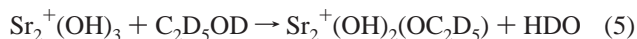
equal intensities, and the abundance of Sr^+PrOH was greater than that of Sr^+PrO .

Reactions of metal oxides and hydroxides with alcohols are known to occur in the condensed phase,³¹ resulting in the formation of metal alkoxides and the release of water. For alkaline earth metals, these reactions can be summarized as



Each reaction is reversible, and because the equilibrium constants are small, water has to be removed continuously during the reaction to obtain high yields of the alkoxide products.³¹ Likewise, ionic oxide and hydroxide clusters of the Group 2A metals should be expected to undergo similar reactions with alcohols. One of the objectives behind studying these reactions was that of confirming earlier assumptions regarding the structures of products formed from the reactions of M_n^+ with water.

With the trap containing the ions Sr_2^+ , Sr_2^+O , $\text{Sr}_2^+\text{O}(\text{OH})$, and $\text{Sr}_2^+(\text{OH})_3$, Figure 3c–e shows the chemical evolution of this population as the concentration of deuterated ethanol in the trap increases. Ethanol vapor was pulsed into the trap via a Jordan nozzle, which meant that the concentration of alcohol could be controlled independently of that of the other reactive species present in the experiment. As can be seen from Figure 3, hydroxyl groups on the strontium-containing complexes gradually undergo exchange to OC_2D_5 . The reaction sequence can be summarized as follows:



As with the condensed-phase analogue,³¹ it is assumed that a whole water molecule rather than $\text{H} + \text{OH}$ is lost following each reactive step. Each of the intermediates in reactions 5–7 can be identified in the mass spectra (Figure 3). From a study of reactions involving both $\text{C}_2\text{D}_5\text{OD}$ and CD_3OD , it has been possible to conclude that the reactions consist of the substitution of OH for OR rather than the replacement of a water molecule by an alcohol. No reactions between ethanol and either Sr^+ , Sr_2^+O , or $\text{Sr}_2^+\text{O}(\text{OH})$ appear to be taking place. Similar substitution steps have been observed for $\text{M}_n^+(\text{OH})_{2n-1}$ with MeO , EtO , and 1-PrO in reactions with methanol, ethanol, and propanol, respectively, M_n^+ being composed of either calcium ($n < 6$), strontium ($n < 5$), or barium ($n < 4$). No complexes with more alkoxide groups than is required by the empirical formula $\text{M}_n^+(\text{OR})_{2n-1}$ were found in any of the mass spectra. Figure 4 shows examples of how reaction products evolve following the introduction of deuterated methanol into a trap containing just $\text{Sr}_n^+(\text{OH})_{2n-1}$ complexes. Obviously, the range of complexes that can be studied is influenced by the upper mass limit of the trap (650 amu). As seen previously for the hydroxide complexes, all ions of the form $\text{M}_n^+(\text{OH})_{2n-1-m}(\text{OR})_m$ display a marked resistance to fragmentation following collisional activation. Such behavior again supports the assumption that neither water nor alcohol adducts are present in the structure of the complexes.

It is not quite clear, however, why bare and suboxide cluster ions such as Sr_2^+ and Sr_2^+O do not react with alcohols in a manner similar to that seen for the monatomic metal ions. It can only be assumed that these reactions must be much slower than the reactions with water vapor residing in the trap. Only $\text{Ba}_2^+\text{O}(\text{OH})$ reacts with ROH to form $\text{Ba}_2^+\text{O}(\text{OH})\text{ROH}$. A further reaction with alcohol results in the production of $\text{Ba}_2^+\text{O}(\text{OH})(\text{RO})_2$ and $\text{Ba}_2^+(\text{RO})_3$. This observation could imply that $\text{Ba}_2^+\text{O}(\text{OH})\text{ROH}$ adopts a $\text{Ba}_2^+(\text{OH})_2\text{RO}$ structure via an intercluster rearrangement in order to follow the route described by reactions 6 and 7.

Given the calculated structures shown for $\text{Ca}_2^+(\text{OH})_3$ and $\text{Ca}_3^+(\text{OH})_5$ in Figures 5 and 6, it is not immediately obvious how the exchange mechanism with OR groups might operate. One possibility for $\text{Ca}_2^+(\text{OH})_3$ as shown in Figure 5 is for the terminal OH groups to be displaced, which could then lead to a structural rearrangement revealing the OH group that is held between the two calcium atoms. It is clear from the events shown in Figure 4 that the exchange process is both comparatively slow and sequential, which would allow for the possibility of structural rearrangement. Likewise, for $\text{Ca}_3^+(\text{OH})_5$, the two out-of-plane OH groups shown in Figure 6 could be displaced, again leading to a structural rearrangement that would make the remaining groups more amenable to substitution.

V. Conclusions

Formation of the stoichiometric hydroxide clusters $\text{M}_n^+(\text{OH})_{2n-1}$ has been observed in the reactions of ionic clusters of calcium ($n = 2-6$), strontium ($n = 2-5$), and barium ($n = 2, 3$) with water molecules. For calcium, the other products of these reactions are $\text{Ca}_n^+\text{O}(\text{OH})_{2n-3}$, and their stability increases with n with respect to that of $\text{Ca}_n^+(\text{OH})_{2n-1}$. Stoichiometric $\text{Sr}_n^+\text{O}_{n-1}\text{OH}$, for $n = 2, 4$, and 6, and $\text{Sr}_n^+\text{O}_{n-2}(\text{OH})_3$, for $n = 3$ and 5, complexes are also formed in the reaction of Sr_n^+ with water. The formation of Ba_4^+O_4 ions previously reported in our TOF MS study has been confirmed using an ion trap, and the formation of Ba_3^+O_4 has also been observed. Reactions between $\text{M}_n^+(\text{OH})_{2n-1}$ and alcohols ROH result in sequential substitution of hydroxyl groups for OR until the complexes $\text{M}_n^+(\text{OR})_{2n-1}$ are formed. The ionic oxide and mixed oxide–hydroxide clusters seem to be less reactive toward alcohols than stoichiometric hydroxide clusters $\text{M}_n^+(\text{OH})_{2n-1}$.

Acknowledgment. We thank Mitchell Lee Meade for assistance with some of the experiments, Dr. Andrei Protchenko for helpful discussions, and Dr. Perdita Barran for discussions and critical reading of the manuscript. We also acknowledge EPSRC for financial support and the award of a studentship to G.A.-B.

References and Notes

- (1) Baes, C. F.; Mesmer, R. E. *The Hydrolysis of Cations*; Wiley: New York, 1969.
- (2) Misaizu, F.; Sanekata, M.; Fuke, K.; Iwata, S. *J. Chem. Phys.* **1994**, *100*, 1161.
- (3) Sanekata, M.; Misaizu, F.; Fuke, K.; Iwata, S.; Hashimoto, K. *J. Am. Chem. Soc.* **1995**, *117*, 747.
- (4) Harms, A. C.; Khanna, S. N.; Chen, B.; Castleman, A. W., Jr. *J. Chem. Phys.* **1994**, *100*, 3540.
- (5) Watanabe, H.; Iwata, S. *J. Phys. Chem. A* **1997**, *101*, 487.
- (6) Sperry, D. C.; Midey, A. J.; Lee, J. I.; Qian, J.; Farrar, J. M. *J. Chem. Phys.* **1999**, *111*, 8469.
- (7) Watanabe, H.; Iwata, S.; Hashimoto, K.; Fuke, K.; Misaizu, F. *J. Am. Chem. Soc.* **1995**, *117*, 755.
- (8) Lu, W.; Yang, S. *J. Phys. Chem. A* **1998**, *102*, 825.
- (9) Mikhailov, V. A.; Barran, P. E.; Stace, A. *J. Phys. Chem. Chem. Phys.* **1999**, *1*, 3461.

- (10) Boutou, V.; Lebeault, M. A.; Allouche, A. R.; Pauling, F.; Viallon, J.; Bordas, C.; Chevaleyre, J. *J. Chem. Phys.* **2000**, *112*, 6228.
- (11) Schweikhard, L.; Krückeberg, S.; Lutzenkirchen, K.; Walther, C. *Eur. Phys. J. D* **1999**, *9*, 15.
- (12) Beyer, M.; Berg, C.; Görlitzer, H. W.; Schindler, T.; Achatz, U.; Albert, G.; Niedner-Schatteburg, G.; Bondybey, V. E. *J. Am. Chem. Soc.* **1996**, *118*, 7386.
- (13) Hanratty, M. A.; Paulsen, C. M.; Beachamp, J. L. *J. Am. Chem. Soc.* **1985**, *107*, 5074.
- (14) Dietrich, G.; Krückeberg, S.; Lutzenkirchen, K.; Schweikhard, L.; Walther, C. *J. Chem. Phys.* **2000**, *112*, 752.
- (15) Kirkwood, D. A.; Stace, A. J. *J. Am. Chem. Soc.* **1998**, *120*, 12316.
- (16) Odeney, M. D. *Philos. Thesis*, The University of Sussex, Falmer, U.K., 1999.
- (17) Guan, S.; Marshall, A. G. *J. Am. Soc. Mass Spectrom.* **1996**, *7*, 101.
- (18) Mirick, J. W.; Chien, C.-H.; Blaisten-Barojas, E. *Phys. Rev. A* **2001**, *63*, 023202.
- (19) Kirschner, K. N. *J. Chem. Phys.* **2000**, *112*, 10228. Alcamí, M.; González, A. I.; Mó, O.; Yáñez, M. *Chem. Phys. Lett.* **1999**, *307*, 244. Kirschner, K. N.; Ma, B.; Bowen, J. P.; Duncan, M. A. *Chem. Phys. Lett.* **1998**, *295*, 204.
- (20) Baerends, E. J.; Ellis, D. E.; Ros, P. *Chem. Phys.* **1973**, *2*, 41.
- Versluis, L.; Ziegler, T. *J. Chem. Phys.* **1988**, *88*, 322. te Velde, G.; Baerends, E. J. *J. Comput. Phys.* **1992**, *99*, 84. Fonseca Guerra, C.; Snijders, J. G.; te Velde, G.; Baerends, E. J. *Theor. Chem. Acc.* **1998**, *99*, 391.
- (21) Vosko, S. H.; Wilk, L.; Nusair, M. *Can. J. Phys.* **1980**, *58*, 1200.
- (22) Becke, A. D. *Phys. Rev. A* **1988**, *38*, 2098.
- (23) Perdew, J. P. *Phys. Rev. B* **1986**, *33*, 8822.
- (24) Fan, L.; Ziegler, T. *J. Chem. Phys.* **1992**, *96*, 9005.
- (25) Partridge, H.; Langhoff, S. R.; Bauschlicher, C. W. *J. Chem. Phys.* **1986**, *84*, 4489.
- (26) Bauschlicher, C. W.; Sodupe, M.; Partridge, H. *J. Chem. Phys.* **1992**, *96*, 4453.
- (27) Vol'nov, I. I. In *Peroxides, Superoxides, and Ozonides of Alkali and Alkaline Earth Metals*; Petrocelli, A.W., Ed.; Plenum Press: New York, 1966.
- (28) Liptrop, G. F. *Modern Inorganic Chemistry*; Bell & Hyman: London, 1985.
- (29) Felmy, A. R.; Dixon, D. A.; Rustad, J. R.; Mason, M. J.; Onishi, L. M. *J. Chem. Thermodyn.* **1998**, *30*, 1103.
- (30) Baes, C. F., Jr.; Mesmer, R. E. *The Hydrolysis of Cations*; Wiley: New York, 1969; p 420
- (31) Bradley, D. C.; Mehrotra, R. C.; Gaur, D. P. *Metal Alkoxides*; Academic Press: London, 1978.